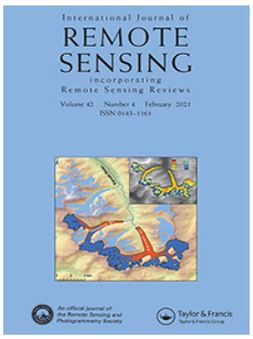

International Journal of Remote Sensing

ISSN: 0143-1161 (Print) 1366-5901 (Online) Journal homepage: www.tandfonline.com/journals/tres20

Investigation of seasonal variability of atmospheric columnar CO_2 over India in relation to environmental parameters using OCO-2 observation and vertical redistribution model

Barun Raychaudhuri & Santanu Roy

To cite this article: Barun Raychaudhuri & Santanu Roy (2021) Investigation of seasonal variability of atmospheric columnar CO_2 over India in relation to environmental parameters using OCO-2 observation and vertical redistribution model, International Journal of Remote Sensing, 42:4, 1450-1473, DOI: 10.1080/01431161.2020.1832281

To link to this article: https://doi.org/10.1080/01431161.2020.1832281

Published online: 07 Dec 2020.

INTERNATIONAL JOURNAL OF REMOTE SENSING
2021, VOL. 42, NO. 4, 1450–1473
https://doi.org/10.1080/01431161.2020.1832281

Taylor & Francis
Taylor & Francis Group

Investigation of seasonal variability of atmospheric columnar CO_2 over India in relation to environmental parameters using OCO-2 observation and vertical redistribution model

Barun Raychaudhuri and Santanu Roy

Department of Physics, Presidency University, Kolkata, India

ABSTRACT

This work re-explores the seasonal change of atmospheric carbon dioxide (CO_2) concentration, a subject of renewable interest over half a century, in both time and frequency domain and identifies the atmospheric surface pressure and the surface air temperature as key factors for the temporal variation. The annual variability of CO_2 dry-air mole fraction derived from the National Aeronautics and Space Administration Jet Propulsion Laboratory (NASA-JPL) Orbiting Carbon Observatory-2 (OCO-2) database for the region bounded by 22° N to 23° N and 86° E to 89° E was found to increase in summer, to decrease in winter and to exhibit a tendency of increase at the end of the year consistently for the years 2016 and 2017 whereas the corresponding variations of solar-induced fluorescence, surface pressure and air temperature showed partial consistency with that. The trends of these findings were cross-checked with the long-time gross variations of CO_2, Normalized Difference Vegetation Index, surface pressure and surface temperature for 25 urban regions within approximately 20° N to 29° N and 69° E to 89° E obtained from NASA-Giovanni database for a period of 2010 to 2017. The periodic variations of these parameters were pin-pointed by Fourier transform. Field measurements were carried out for ground level and column-averaged CO_2 concentrations in parts per million (ppm) at the region around Kolkata city (22.55° N, 88.35° E). Based on the above findings, a simple atmospheric model is developed for vertical redistribution of CO_2 molecules under changed temperature and pressure causing a changed atmospheric path for radiation absorption and an apparent change in the gas concentration at any specific altitude.

ARTICLE HISTORY
Received 26 January 2020
Accepted 15 September 2020

1. Introduction

The monitoring of atmospheric carbon dioxide (CO_2), an important greenhouse gas has got tremendous impetus during the last few decades through the application of ground-based (Wunch et al. 2011; Andrews et al. 2014; Buschmann et al. 2016), airborne (Green 2001; Dennison et al. 2013) and satellite-borne (Bovensmann et al. 1999; Hamazaki, Kaneko, and Kuze 2004; Crisp et al. 2004; Kuze et al. 2009; Wei et al. 2014; Frankenberg et al. 2015; Watanabe et al. 2015; Crisp et al. 2017) sensors. The comparisons of such

CONTACT Barun Raychaudhuri barun.physics@presiuniv.ac.in Department of Physics, Presidency University, Kolkata 700073, India

measurements are also studied (Buschmann et al. 2016; Wunch et al. 2017). Reports are available on global (Machida et al. 2008; Yoshida et al. 2011; Crisp et al. 2017), regional (Tiwari, Revadekar, and Ravi Kumar 2013; Tiwari et al. 2014; Ravi Kumar, Revadekar, and Tiwari 2014, 2016; Hakkarainen, Ialongo, and Tamminen 2016; Umezawa et al. 2018; Gupta et al. 2019) and local (Huang et al. 2015; Xueref-Remy et al. 2018; Imasu and Tanabe 2018; Roman-Cascon et al., 2019) CO_2 assessments.

The general trend of the temporal variation of atmospheric CO_2 concentration exhibits a continuous increase with time superimposed by an oscillatory seasonal change (Keeling et al. 1976, 2005; Basu et al. 2014; Imasu and Tanabe 2018). Generally, the amplitude of the annual change is found to be more predominant in the northern hemisphere than that in the southern hemisphere (Dettinger and Ghil 1998; Keeling et al. 2005; Jiang et al. 2016). As obvious, the seasonal variation of atmospheric CO_2 concentration has been a well-observed phenomenon for almost half a century. The seasonal growth of terrestrial vegetation causing consumption and release of CO_2 is affirmed to be the reason for such periodic change (Keeling, Chin, and Whorf 1996; Buermann et al. 2007; Basu et al. 2014).

However, other interesting features related to the CO_2 concentration are testified simultaneously all the way thereby sustaining the appeal of the topic. The occurrence of the maximum and the minimum of CO_2 concentration at two different seasons for northern and southern hemispheres (Monfray et al. 1987; Nevison et al. 2008), semi-annual fluctuation (Jiang et al. 2016) and simulated effect of fossil fuel emission on the sub-annual variation (Zhang et al. 2016) of CO_2 concentration, effects of Madden-Julian Oscillation (Li et al. 2010) and El Nino events (Keeling, Chin, and Whorf 1996; Nevison et al. 2008; Jiang et al. 2013) on the CO_2 concentration are several such examples. The greenhouse contribution of CO_2 and related global climate changes (Kondratyev and Varotsos 1995), long-range persistence in the fluctuation of CO_2 concentration (Varotsos, Assimakopoulos, and Efstathiou 2007) and atmosphere-ocean CO_2 exchange (Krapivin and Varotsos 2016) are studied. There exist reports on the link between CO_2 and climate variability, such as rainfall (Tiwari, Revadekar, and Ravi Kumar 2013) and sea surface temperature (Ravi Kumar et al. 2016), spatial variability (Tiwari et al. 2014), interannual variability of tropical carbon balance in response to climate-driven variations (Fu et al. 2017) and the role of non-uniform climate warming on the seasonal cycle of CO_2 variation (Li et al. 2018).

Recent studies on CO_2 seasonal changes include diversified elements, such as correlation of climatic influence with gross primary production (GPP) (Lee et al. 2018), biosphere and anthropogenic seasonal CO_2 contributions (Xueref-Remy et al. 2018), seasonal variability of CO_2 partial pressure in waterbody (Marescaux et al. 2018) and the influence of wind direction (Román-Cascón et al. 2019) on CO_2 mixing ratio. The concern about the consensus on the main factors increasing CO_2 seasonal amplitude (Piao et al. 2018) and the attempts to predict its future trend (Zhao and Zeng 2014) reiterate the importance of the topic.

The above outline put forward some candid questions. The seasonal fluctuation of CO_2 is well known but what is the actual nature of the oscillation is not so well defined. When the global mean variation over large area is observed, it appears like almost sinusoidal but not mathematically affirmed. When a smaller local area is considered, the oscillation goes far from sinusoidal. Plenty of both types of variations are reported (Keeling 1976; Monfray

1987; Dettinger and Ghil 1998, Keeling 2005; Basu 2014; Imasu 2018) but surprisingly the actual periodicity is unexplained. A complicated sum of polynomial and harmonics is sometimes proposed to track the seasonal variation (Nevison 2008).

The objectives of the present work are to explore the trend of the seasonal periodic variation of atmospheric CO_2 throughout the year both in time and frequency domain, to find out the origin of such variation and to provide with a suitable atmospheric model to explain the phenomena. The study region comprises several plain areas of north India with tropical climate and varying vegetation extent and urban congestion. The study involves the seasonal variation of atmospheric CO_2 concentration (ppm) along with that of vegetation activities and atmospheric pressure and temperature. Initially the seasonal changes of CO_2 along with that of solar-induced fluorescence (SIF), surface pressure and air temperature were investigated for a specific region of 1° × 3° (Latitude × Longitude) extension for consecutive 2 years using Orbiting Carbon Observatory-2 (OCO-2) data. The investigations were then generalized for a number of urban places over 9° × 20° (Latitude × Longitude) extension of similar atmospheric conditions using the National Aeronautics and Space Administration (NASA)-Giovanni data on the monthly averages of CO_2 concentration with the corresponding Normalized Difference Vegetation Index (NDVI) and surface pressure and temperature. Field spectro-radiometry was carried out at specific sites and the atmospheric CO_2 concentration in parts per million (ppm) was derived from the same. Based on these satellite data and ground spectroradiometry, the present work explains the influence of atmospheric pressure on the annual variability of CO_2 column average and develops an explanatory model for vertical redistribution of CO_2 molecules.

2. Data and methodology

This work establishes a model for redistribution of atmospheric CO_2 concentration using satellite data analysis and ground spectroscopy. The different parts of the methodology are presented below.

2.1. Satellite data

The following sources of database were used for CO_2 analysis: (i) Orbiting Carbon Observatory 2 (OCO-2) and Atmospheric Infrared Sounder (AIRS) day-wise CO_2 data produced by the Jet Propulsion Laboratory, California Institute of Technology and archived by the NASA Goddard Earth Science Data and Information Services Center (https://oco.jpl.nasa.gov/oco-2-data-centre/) and (ii) monthly averaged atmospheric CO_2, NDVI, surface pressure, and surface air temperature data (Table 1) from NASA Giovanni online environment geophysical parameter (https://giovanni.gsfc.nasa.gov/giovanni/).

It is worthwhile to mention that OCO-2 detects CO_2 at two absorption bands centred about 1.61 μm and 2.06 μm, referred to as 'weak absorption' and 'strong absorption', respectively (Crisp et al. 2017) whereas AIRS retrieves CO_2 utilizing 15 μm band of the spectrum (Wei et al. 2014). The details of estimating the column-averaged concentration of atmospheric CO_2 and SIF from the spectroscopy of the reflected solar radiation are available in literature (Frankenberg et al. 2012; Sun et al. 2018). It may be mentioned that

Table 1. Specification of parameters downloaded from NASA Giovanni online environment.

Parameter	Source	Temporal resolution	Spatial resolution (°)
Carbon dioxide, mole fraction in free troposphere, infrared only	Atmospheric Infrared Sounder Earth Observing System (AIRS EOS) Aqua satellite sensor	Monthly	2.5 × 2.0
NDVI	Moderate Resolution Imaging Spectroradiometer (MODIS)-Terra satellite sensor	Monthly	0.05 × 0.05
Surface air pressure	Global Land Data Assimilation System Version 2 (GLDAS-2) surface observation and model-based re-analysis /data assimilation system	Monthly	0.25 × 0.25
Surface air temperature	Modern-Era Retrospective analysis for Research and Applications, Version 2 (MERRA-2) surface observation and model-based re-analysis/data assimilation system	Monthly	0.500 × 0.625

the CO_2 exchange with vegetation during photosynthesis, quantified as GPP is positively related with SIF (Joiner et al. 2014; Miao et al. 2018).

The day-wise column-averaged CO_2 dry-air mole fraction (xCO_2) values were extracted from OCO-2 database for both the above mentioned weak and strong CO_2 bands for the region bounded by 22° N to 23° N and 86° E to 89° E for two consecutive years; 2016 and 2017. The region under study was a plain area of moderate tropical wet-and-dry climate and uniform seasonal variation over the years having surface vegetation around 66%, land use to land cover ratio around 4:5 (Source: same as that of Table 2). Kolkata city (West Bengal State, India), having monthly mean temperature of 19 to 30°C is situated within this region and consists of the sites of ground-level spectroscopic measurements (subsection 2.2). Three other parameters, namely SIF, surface pressure and surface temperature were also extracted for the same specified region and time span. The AIRS CO_2 data were analysed for the year 2010 for both daytime and night-time.

In order to study the average trend of variation of CO_2 concentration over an wider area of comparable climate, the monthly average values of AIRS-derived CO_2 mole fraction (ppm) at Kolkata and 24 other urban areas of India within approximately 20° N to 29° N and 69° E to 89° E (Figure 1 and Table 2) were procured from NASA-Giovanni

Table 2. Land use land cover information for the states containing the 25 places of Figure 1 for obtaining CO_2 monthly average data (Source: calculated from the statistics of 2015 to 2016 provided by *Bhuvan*, Indian Geo-Platform of Indian Space Research Organization, National Remote Sensing Centre, India (https://bhuvan-app1.nrsc.gov.in/thematic/thematic/index.php).

		Different geographic features (%)				
Name of the state	Site numbers of Figure 1 contained	Agriculture	Barren	Built up	Forrest/ Grass	Waterbody/ Wetland/ Snow
Bihar	16	77.29	2.87	6.98	6.26	6.60
Chattisgarh	4, 17, 23	45.74	2.71	3.31	45.70	2.54
Delhi	5	34.66	5.09	57.36	1.00	1.89
Gujarat	1, 11, 20, 21	62.06	21.56	2.84	6.72	6.82
Jharkhand	6, 12	50.01	7.08	5.72	34.60	2.59
Madhya Pradesh	2, 7, 8, 19, 25	61.04	8.06	1.86	26.15	2.89
Odisha	3, 18, 24	50.85	7.19	4.16	33.14	4.66
Rajasthan	9	67.96	19.13	1.70	9.28	1.93
Uttar Pradesh	14, 15, 22	80.73	3.09	5.31	6.48	4.39
West Bengal	10, 13	61.04	1.32	18.08	11.27	8.29

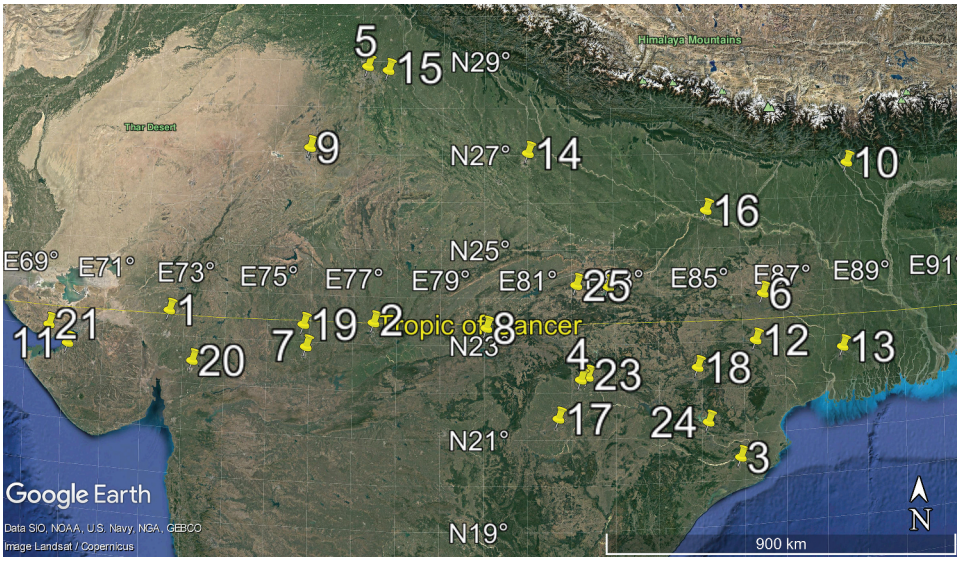

Figure 1. Urban places of India for obtaining CO_2 monthly average data from NASA- Giovanni online environment, locations indicated as: 1. Ahmedabad, 2. Bhopal, 3. Bhubaneswar, 4. Bilaspur, 5. Delhi, 6. Dhanbad, 7. Indore, 8. Jabalpur, 9. Jaipur. 10. Jalpaiguri, 11. Jamnagar, 12. Jamshedpur, 13. Kolkata, 14. Lucknow, 15. NTPC Dadri, 16. Patna, 17. Raipur, 18. Rourkela, 19. Ujjain, 20. Vadodara and thermal power stations of 21. Mundra, 22. Rihand, 23. Sipat, 24. Talcher, 25. Vindhyachal.

site for the period of January, 2010 to December, 2017. These places have the similarities of being plain, urban area under similar tropical climate and have dissimilarities in the extent of vegetation and possible CO_2 emission, as expected from Table 2. Several thermal power plants are also included in the wide choice of regions. The average temporal variation was fitted linearly and the linear increase was subtracted from each datum to retain only the seasonal fluctuation component riding over the initial value. Three other parameters, namely NDVI, surface pressure, and surface air temperature were procured from the same source for the same regions and for the same period, as specified in Table 1. These parameters were chosen because the NDVI is considered as an indicator of vegetation activity in carbon uptake through photosynthesis (Gamon et al. 1995; Nestola et al. 2016). However, the SIF occurs due to chlorophyll alone while the NDVI contains the combined contribution of other leaf tissues and canopy structure and cannot be correlated directly with CO_2 removal by photosynthesis. The possible effects of atmospheric pressure and temperature were anticipated from the review of the earlier studies mentioned in Section 1.

2.2. Ground measurements

The objective of this measurement was to correlate the column-averaged concentration of CO_2 with that at surface level. The solar spectral irradiance were measured at different places of Kolkata city (around 22.55° N, 88.35° E) under cloud-free solar illumination throughout the ultraviolet-visible-shortwave infrared wavelength range with Analytical Spectral Devices (ASD) spectroradiometer having spectral sampling interval of 1.4 nm for

350 to 1000 nm and 2 nm for 1000 to 2500 nm. The instrument held vertically upward was fitted with wide angle (Field of View 180°) remote cosine receptor on the fibre of 25° Field of View. At the same time, the local concentrations (ppm) of atmospheric CO_2 at the ground surface were measured with handheld carbon dioxide metre Model GCH-2018. Different urban places of widely varying population density and vehicle abundance were chosen deliberately for the measurements. Two carbon dioxide absorption bands, henceforth designated as CO_2-1 and CO_2-2 were obtained around 2 μm on the ground-based solar irradiance spectra. The CO_2 concentrations (ppm) were estimated from those absorption depths using the standard differential optical absorption spectroscopic (DOAS) technique.

2.3. Mathematical model for CO_2 redistribution

A simple model is developed to explain the change of CO_2 concentration at an arbitrary altitude with respect to that at the ground surface due to change in temperature, hence pressure. As obtained from literature (Sawyer 1972; Berner 2003; Queißer, Burton, and Kazahaya 2019), the net atmospheric CO_2 is the consequence of the simultaneous effects of the chief sources, such as human activities, volcanic eruption and biosphere respiration, the major sinks, such as vegetation, ocean and soil and the complex feedback from organic matter. Majority of the above entities belong to the earth surface. The vertical diffusion of the emitted CO_2 gradually changes its average amount over the whole atmospheric column. Being chemically less reactive, CO_2 persists in the atmosphere for a long time and both its sequestration to sinks and mixing with air are very slow processes. Considering the above scenario, the total number density $N(z)$ of atmospheric CO_2 molecules present at an arbitrary altitude z at a certain instant of time may be expressed as the combination of two components:

$$N(z) = n(z) + \upsilon(z) \tag{1}$$

$n(z)$ representing the number density of CO_2 molecules well-mixed with air and governed by the instantaneous atmospheric pressure and temperature and $\upsilon(z)$ denoting the randomly varying net amount of CO_2 molecules supplied by the sources and taken up by the sinks. The second component is not uniformly assimilated in the air, does not obey the instantaneous air pressure and temperature and accounts for the random vertical change of CO_2 molecules due to the gradual diffusion of surface air throughout the atmosphere.

Assuming the ideal gas law for air, the rate of change of the partial pressure (P) of CO_2 with altitude (z) can be expressed as

$$\frac{dP}{dz} = -\chi\rho_0 g \tag{2}$$

where$\rho_0 = (P \times M)/(R_G \times T)$is the equilibrium density of CO_2, g = 9.8 m s^{-2} is the acceleration due to gravity, $M = 44 \times 10^{-3}$ kg mol^{-1} is the molecular weight of CO_2, R_G = 8.31 J K^{-1} mol^{-1} is the gas constant, T is the atmospheric temperature (K) and χ is a dimensionless constant accounting for the fluctuation in density profile. If χ becomes unity, the rate of change of pressure with altitude in ideal condition is obtained. The smaller is the value of χ, the sharper is the variation of pressure with altitude. The height

dependent, hence pressure-dependent number density of CO_2 can be expressed as $n(z) = (A \times P)/(R_G \times T)$ where $A = 6.023 \times 10^{23}$ molecules mol^{-1} is the Avogadro number. Using Equation (2) and the related expressions, one can obtain, at an arbitrary temperature,

$$\frac{dn(z)}{n(z)} = -\chi\left(\frac{gM}{R_G T}\right)dz \tag{3}$$

which can be integrated over the altitude to get the number density of CO_2 molecules as function of altitude. Considering standard linear decrease of atmospheric temperature (T) with altitude within the troposphere (Elachi and van Zyl 2006) as $T = T_0 - \alpha \times z$, T_0 being the equilibrium surface temperature and α a constant lapse rate (K m^{-1}), the integral representing the pressure-dependent number density of CO_2 mixed in air at altitude z is obtained as

$$n(z) = n_0\left(1 - \frac{\alpha z}{T_0}\right)^k \tag{4}$$

where n_0 is the number density at ground level and

$$k = \left(\frac{\chi g M}{\alpha R_G}\right) \tag{5}$$

is a dimensionless constant quantity. At a certain maximum altitude, the number of CO_2 molecules becomes almost zero. It is the case when the term $\left(1 - \frac{\alpha z}{T_0}\right)$ in Equation (4) becomes almost zero, i.e. z becomes almost T_0/α. For instance, assuming T_0 = 300 K and α = 0.0065 K m^{-1}, z is about 45 km. The generality of Equation (4) can be interpreted as follows. It is obvious from the above mentioned standard values of parameters that k □ 1. Assuming $k \to \infty$ and using the identity $\lim_{k\to\infty}(1 + x/k)^k \to \exp(x)$, Equation (4) can be approximated as

$$n(z) = n_0 \exp\left(-\frac{\chi z}{H}\right) \tag{6}$$

which is similar to the ideal case of exponential decrease of atmospheric air molecular density with altitude (Elachi and van Zyl 2006) where $H = (R_G \times T_0)/(g \times M)$= 5.78 km can be designated as the scale height for CO_2. Moreover, $n(z)$ represents the number of CO_2 molecules per unit volume of air and is proportional to its mole fraction [$xCO_{2(z)}$] at altitude z. Consequently Equation (4) can be further modified in terms of the mole fraction as

$$xCO_{2(z)} = xCO_{2(0)} \exp\left(-\frac{\chi z}{H}\right) \tag{7}$$

where $xCO_{2(0)}$ is the mole fraction at ground surface. The present work considers Equation (4) in its original form.

The $\upsilon(z)$ component representing the CO_2 outcome of source-sink interaction and its vertical transport due to diffusion is a random process. Since the dispersion of atmospheric particles due to wind and eddy motion is expressed as Gaussian function of altitude (Stockie 2011), this random value of the unmixed CO_2 suspended in air at an altitude z may be quantified by Gaussian variation over the altitude as

$$\upsilon(z) = \upsilon_h \exp\left[-\frac{(z-h)^2}{\sigma^2}\right] \tag{8}$$

where υ_h is the instantaneous unmixed CO_2 concentration at arbitrary height h ($0 < h < z$) under the average effect of advection by the wind and the parameter σ accounts for the standard deviation of the Gaussian concentration distribution resulting from the eddy variation over the altitude. Any scope for reflection of CO_2 from the ground surface is considered negligible in comparison with the above. The υ_h part of CO_2 is expected to (i) undergo slow change, hence remain unchanged for a certain instant of time and (ii) remain well below the above mentioned upper limit of altitude because there is negligible source of CO_2 above troposphere and lower mixing ratio above 15 to 20 km with strong gradients across the tropopause (Diallo et al. 2017).

Now considering both the above components $n(z)$ and $\upsilon(z)$, the effect of temperature and pressure on the vertical distribution of CO_2 molecules at a certain atmospheric column can be understood. Let n_1 and n_2 be the number densities of CO_2 molecules at the same altitude (z) for two different surface temperatures (T_{01} and T_{02}) and n_{01} and n_{02} be the corresponding ground-level number densities. Let the CO_2 column reaches up to an altitude of z_1 when the ground-level temperature is T_{01}. If this temperature is increased to T_{02}, the same number of CO_2 molecules attains an increased height of z_2 due to decrease in pressure and consequent expansion. The lateral expansion is neglected assuming the neighbouring places being at the same temperature. The integrals of Equation (1) over these two different altitudes should be equal because only the vertical distribution gets changed but the total number of CO_2 molecules reaching two different heights z_1 and z_2 at two different surface temperatures T_{01} and T_{02}, respectively, should remain the same. Therefore,

$$\int_0^{z_1} (n_1 + \upsilon)\mathrm{d}z = \int_0^{z_2} (n_2 + \upsilon)\mathrm{d}z \tag{9}$$

As mentioned above, the activity of $\upsilon(z)$ is slow and remains well below the upper limit of CO_2 column. Consequently, its integrated effect over the altitudes z_1 and z_2 remains the same for both sides and is cancelled out. Thus, on integrating the two sides of Equation (9) and equating the result, the changed number density at ground surface with change in temperature can be obtained in terms of the parameters of Equation (4) as

$$n_{02} = n_{01}\left(\frac{T_{01}}{T_{02}}\right)\frac{1-\left(1-\frac{\alpha z_1}{T_{01}}\right)^{k+1}}{1-\left(1-\frac{\alpha z_2}{T_{02}}\right)^{k+1}} \tag{10}$$

The above combination of Equations (1), (4), (8) and (10) put forward the concept that the seasonal change in surface air temperature can cause change in air pressure so that the expansion or contraction of air can give rise to elevation and redistribution of surface-level CO_2 molecules resulting in an apparent change in the gas concentration at any specific altitude. When the $\left(1-\frac{\alpha z}{T_0}\right)$ terms in Equation (10) tend to zero similar to that of Equation (4), the expression can be simplified as

$$n_{02} = n_{01}\left(\frac{T_{01}}{T_{02}}\right) \tag{11}$$

Using Equations (10) and (11), the corresponding increased height can be related to the initial height as

$$z_2 = z_1\left(\frac{T_{02}}{T_{01}}\right) \tag{12}$$

Equations (11) and (12) state that the redistribution makes the atmospheric path of radiation propagation through the CO_2 molecules longer in comparison with that at lower temperature thereby raising the possibility of undergoing more absorption and yielding apparently higher value of concentration at higher temperature.

The assessment of different relevant parameters used in the above equations are outlined below. Possible numerical values of χ in Equations (5) and (10) were estimated in the following way. Considering the CO_2 column average concentration at Kolkata on the date of the ground measurements, as obtained from OCO-2 data, the altitude profile of tropical atmospheric pressure was simulated with MODTRAN6 software and the slope was determined near the surface. The magnitude of the slope (5.88 to 11.76 Pa m^{-1}) was put to Equation (2) assuming it to be valid for air also with the corresponding values of pressure and density. For air density = 1.2 kg m^{-3} and g = 9.8 m s^{-2}, the value of χ came out to be around 0.7. In the present calculations, it was varied from 0.5 to 1.0. The temperature values for Equations (11) and (12) were obtained from: https://www.timeanddate.com/weather/india/kolkata/climate. The given Celsius values of temperature were converted to absolute (K) values and the mean of the maximum and minimum temperatures of each concerned day was used.

2.3.1. Validation of the model

For the purpose of justifying the above model with respect to CO_2 seasonal variability, the monthly average surface temperature values in India were downloaded from the open data archival of Indian Institute of Tropical Meteorology (https://www.tropmet.res.in/) for years 2000 to 2016, averaged for each month and fitted with third order polynomial to obtain a sample of continuous daily variation throughout a year. For each day, the vertical profile was generated with the above model using the corresponding temperature value. The total CO_2 (ppm) throughout the column was summed up and the percentage of increase/decrease with respect to the minimum was assessed. That accounted for the effect of seasonal variability of temperature, hence that of pressure. However, the actual seasonal variation of CO_2 obtained from OCO-2 or other similar technique gets influenced by at least two more phenomena: a monotonic increase throughout the year due to slow mixing of the surface-emitted CO_2 in the air column and the sequestration caused by vegetation, randomly varying with growth, senescence, and deciduous properties and having a seasonal maximum. The former effect was simulated by adding a linear term [proportional to (1/365) × day] to Equation (1) and the latter one was replicated by subtracting a Gaussian term proportional to exp[– (day – 250)^2/3650] with peak in autumn from Equation (1).

3. Results and discussion

3.1. CO_2 trend and the role of vegetation

The annual variations of CO_2 at the specified region, as obtained from the weak and strong absorption bands for years 2016 and 2017 are displayed in Figure 2. For the local climate, the two ends of the year, namely January and December represent winter season and the middle portion (April-May) represents summer and monsoon seasons. Each point of the graphs, corresponding to a different day stands for an independent recording. As pointed out earlier, the actual mode of the annual variability need to be defined quantitatively. Therefore, to understand the trend of the seasonal variation, the plotted points were tried with second to fifth order polynomials for fitting. The increase in summer, the decrease in autumn and the tendency of increase in the next winter could be fitted with third order polynomial. No significant change was found after the third order. Therefore, all the data points were fitted with third order polynomial, as given in Figure 2. The most prominent feature emerging from all the plots is a tendency of increasing CO_2 concentration in summer season, which is in compliance with some reports (e.g. Basu et al. 2014) but contrary to some others (e.g., Keeling, Chin, and Whorf 1996). Also, there is a tendency to increase the concentration at the end of the year.

In order to cross-check the above nature of CO_2 seasonal variation, the data from AIRS, another independent source, were considered for an earlier period of year 2010 for the

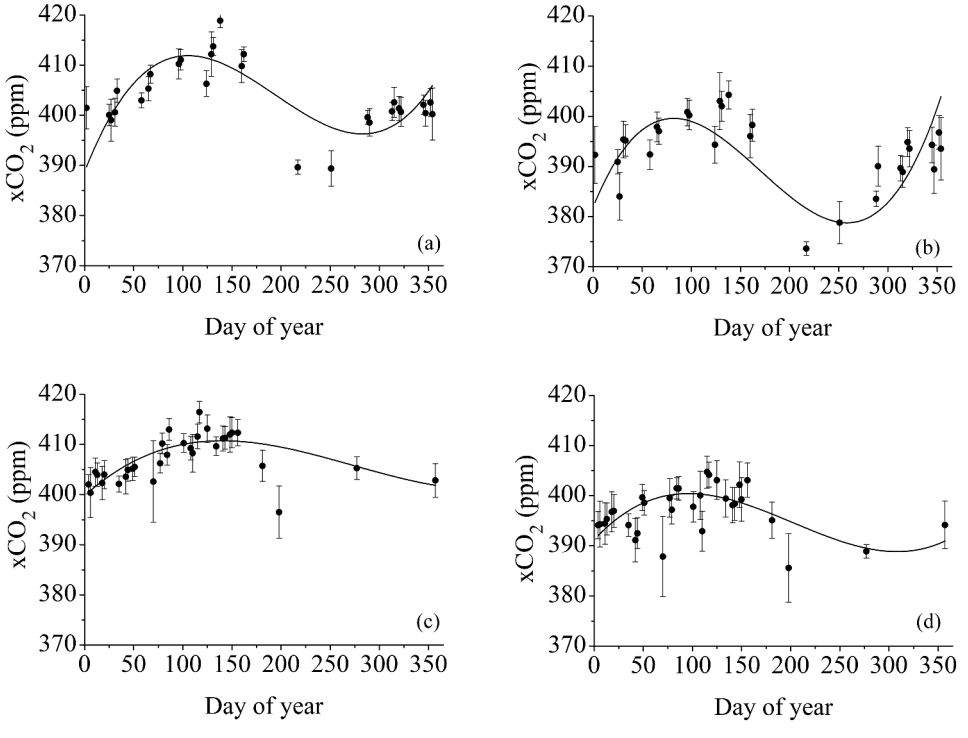

Figure 2. Annual variation of xCO_2 (ppm) for years 2016 and 2017, extracted from OCO-2 database for the weak and strong absorption bands for the region within 22° N to 23° N and 86° E to 89° E, displayed as (a) weak, 2016, (b) strong, 2016, (c) weak, 2017 and (d) strong, 2017.

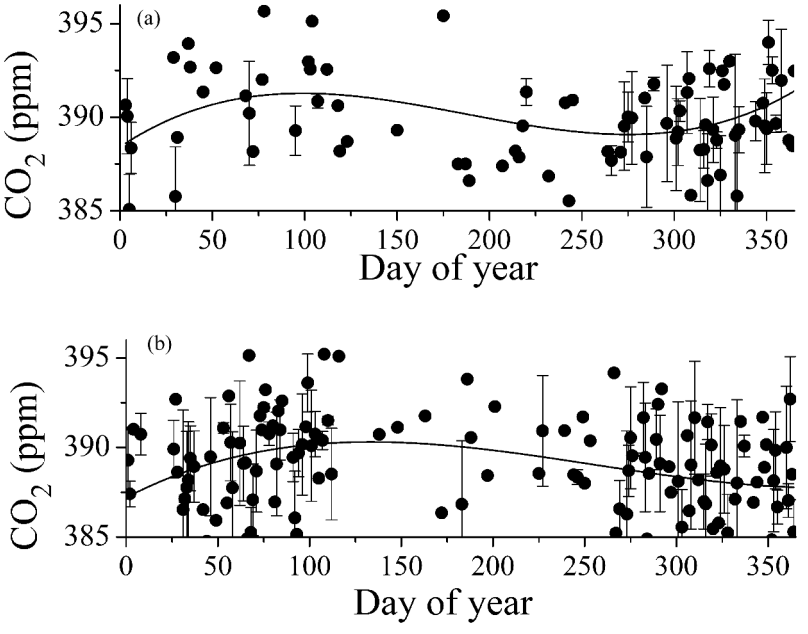

Figure 3. Annual variation of CO_2 concentration (ppm) for (a) Daytime and (b) night-time for year 2010 extracted from AIRS database for the region within 22° N to 23° N and 86° E to 89° E.

region covered in Figure 2. The annual CO_2 change in daytime, as plotted in Figure 3 and fitted with third order polynomial, exhibits a similar increment in summer as that noted in Figure 2. Even the annual change of night-time CO_2 in Figure 3, which is obtained solely from the thermal infrared radiation emitted by the earth in absence of solar radiation shows a weak tendency to increase in summer. The above results approve that the seasonal variation of CO_2 of this region is a characteristic feature irrespective of the observation period and the detecting instrument.

In continuation of the above findings, Figure 4 explores the role of photosynthesis in CO_2 sequestration in terms of SIF of chlorophyll in vegetation. The seasonal variations of SIF obtained from the OCO-2 database for the same region and period as that of Figure 2 are plotted in Figure 4 for the two consecutive years. At the first glance, the trend of the seasonal change of SIF appears to be the 'mirror image' of that of CO_2. The higher SIF corresponds to the lower CO_2 and vice-versa. However, the extent of SIF has remained almost the same during years 2016 and 2017 whereas the CO_2 concentration has increased prominently during the one year. Table 3 compares the present results with an earlier report (Basu at al., 2014) where the seasonal CO_2 variation is found not to synchronize with that of SIF. Thus, although the vegetation activity indicated by SIF is a key reason for CO_2 uptake, the present finding about its seasonal variation is not in full conformity with the seasonal change of CO_2 concentration in atmospheric column, which calls for further investigation.

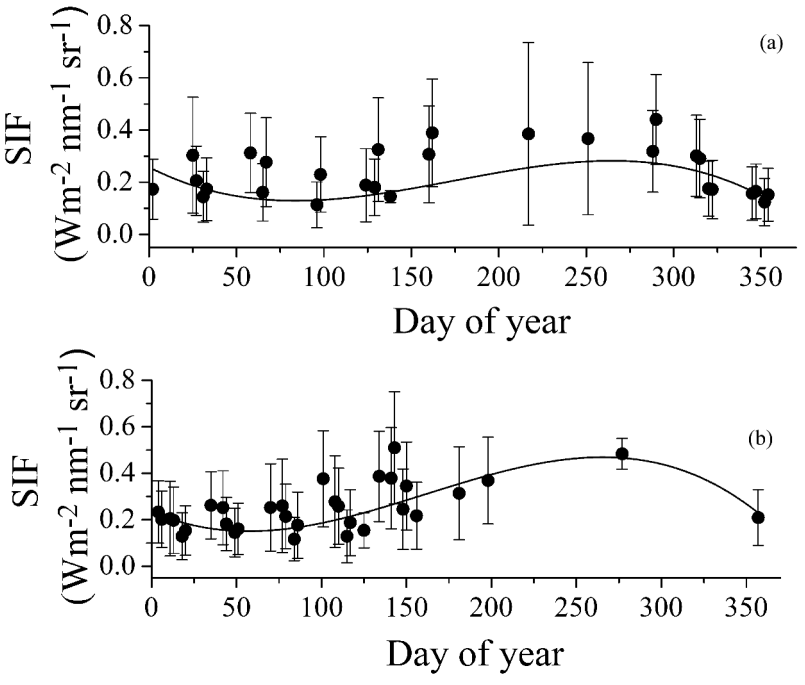

Figure 4. Annual variation of solar-induced fluorescence (Wm^{-2} μm^{-1} sr^{-1}) for years (a) 2016 and (b) 2017, extracted from OCO-2 database for the region within 22° N to 23° N and 86° E to 89° E.

Table 3. Comparison of CO_2 abundance and fluorescence response.

				Approximate seasonal variations	
Reference	Data source	Area	Period	CO_2 (ppm)	Fluorescence (Wm^{-2} sr^{-1} μm^{-1})
Basu et al. 2014	GOSAT, CONTRAIL	Tropical Asia 10° S to 28° N and 80° E to 156° E	January 2009 to September 2011	385 to 393 Max: May Min: September	0.2 to 0.5 Max: July-August Min: December-January
Present work	OCO-2, AIRS and NASA-Giovanni	Tropical urban areas (i) 22° to 23° N and 86° to 89° E (ii) 20° to 29° N and 69° to 89° E approx.	(i) January 2016 to December 2017 (ii) January 2010 to December 2017	395 to 415 Max: April-May Min: August-October	0.1 to 0.6 approx. Max: August-October Min: February-March and December

Abbreviations:
GOSAT: Greenhouse Gases Observing Satellite
CONTRAIL: Comprehensive Observation Network for Trace gases by Airliner

3.2. The role of atmospheric pressure

The above findings on CO_2 seasonal variation compared with the corresponding variation of vegetation vigour revealed that correlating the seasonal growth of terrestrial vegetation to CO_2 uptake is not enough, and the role of some other parameters needs to be explored. Several such reported factors, such as non-uniform warming, wind direction, climatic variability, and surface temperature are mentioned in Section 1. These all are

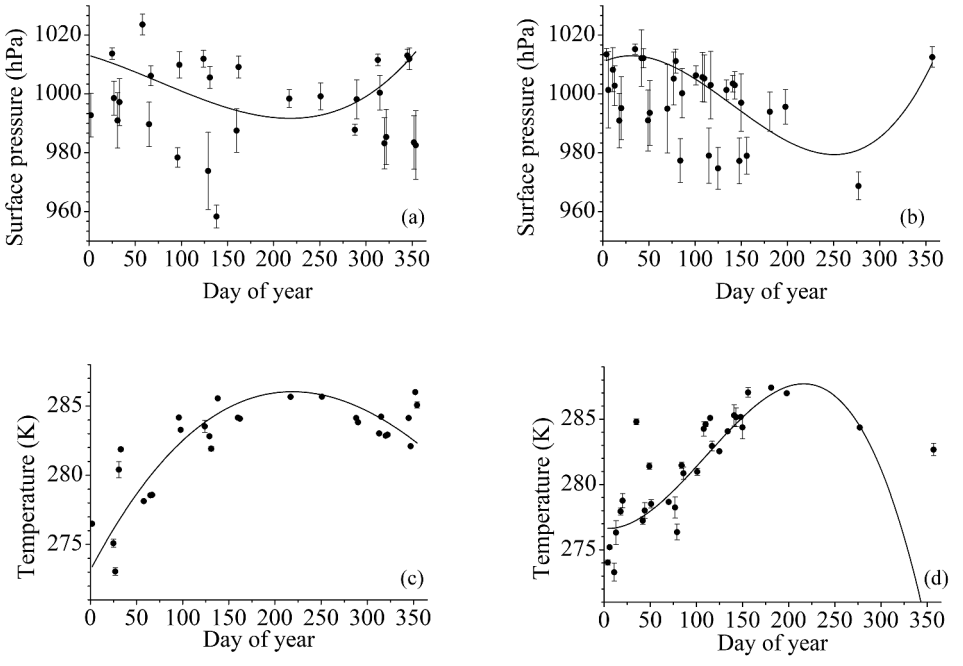

Figure 5. Annual variation of (a) and (b) surface pressure (hPa) and (*c*) and (*d*) air temperature (K) for years 2016 and 2017, respectively, extracted from OCO-2 database for the region within 22° N to 23° N and 86° E to 89° E.

somehow associated with a common entity, namely the atmospheric pressure. Therefore, the effect of atmospheric pressure was verified; first at local scale.

Figure 5 represents the seasonal change of the surface pressure extracted from OCO-2 database for the region and period mentioned in Figure 2. The fundamental gas laws state an inverse relationship between pressure and temperature. Therefore, the corresponding air temperatures obtained from the same data source are also plotted for comparison. It is apparent from Figure 5 that the surface pressure decreases in monsoon and autumn seasons and increases in the winter (two ends of the year). The opposite trend is shown by the surface air temperature.

The trend of seasonal variation of surface pressure does not match that of CO_2 but it is noteworthy that the lowered CO_2 in the winter at the beginning of the year matches the higher surface pressure and up to the summer, these two entities exhibit the opposite tendency. The pressure decreases while the CO_2 increases; as if the lowering of pressure supports the enhancement of CO_2. Thus a strong influence of atmospheric pressure on the seasonal variation of CO_2 concentration is indicated, which is studied for a longer period in the next section.

3.3. Long-term variation of parameters

As the next step, the long duration changes of the above parameters over a large area (Figure 1) were investigated with a view to explore the generalized trends of the seasonal changes. The study for long-term change is initiated with Figure 6, which

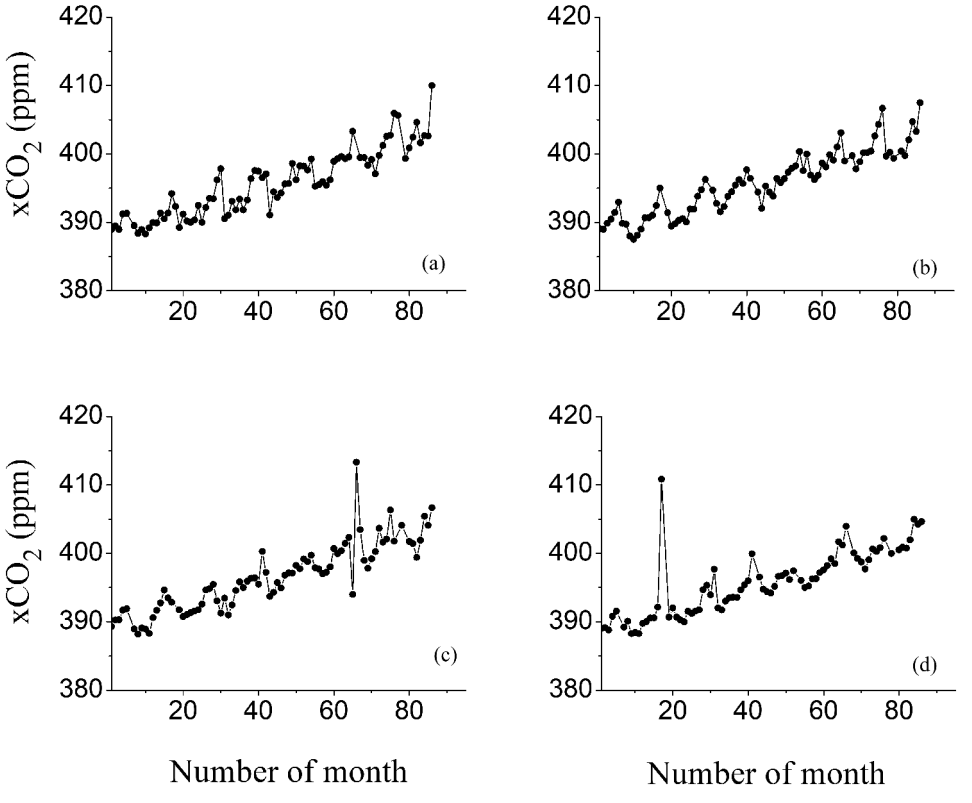

Figure 6. Annual variation of CO_2 concentration over the period of year 2010 to 2017 for four randomly selected places of.Figure 1, namely (a) Ahmedabad (No. 1), (b) Bhopal (No. 2), (c) Delhi (No. 5) and (d) Rourkela (No. 18), obtained from NASA-Giovanni database specified in Table 1

contains the monthly CO_2 variation for four randomly chosen sites from those of Figure 1. Each one undergoes a steady temporal increase with an irregular annual fluctuation superimposed. Then, we move forward to Figure 7(a) where the CO_2 concentration values for all the 25 places are averaged for each month. Comparing with Figure 6 it is noted that the annual periodicity in Figure 7(a) is more prominent and organized. It does not have any regular waveform but exhibits a clear positive trend superimposed by a uniform seasonal cycle. This comparison demonstrates how the global CO_2 variation averaged over vast area assumes a well-defined periodicity. Then, the isolated seasonal fluctuation component (mentioned in Section 2.1) is plotted in Figure 7(b). The corresponding seasonal variations of NDVI values varied widely for the above cities. On averaging over all of those, the periodic change was found to be that of Figure 7(c). It may be noted from Figure 7(b,c) that the CO_2 has a tendency to increase when the NDVI decreases and vice versa. Next, the trend of variation of atmospheric pressure was investigated for the above regions. The monthly values of surface pressure averaged over the mentioned sites for the mentioned period is plotted in Figure 7(d). The corresponding surface air temperature values are given in Figure 7(e). It is quite obvious that the pressure and the temperature vary in opposite phase and comparing Figure 7(b,d,e) it becomes prominent that there

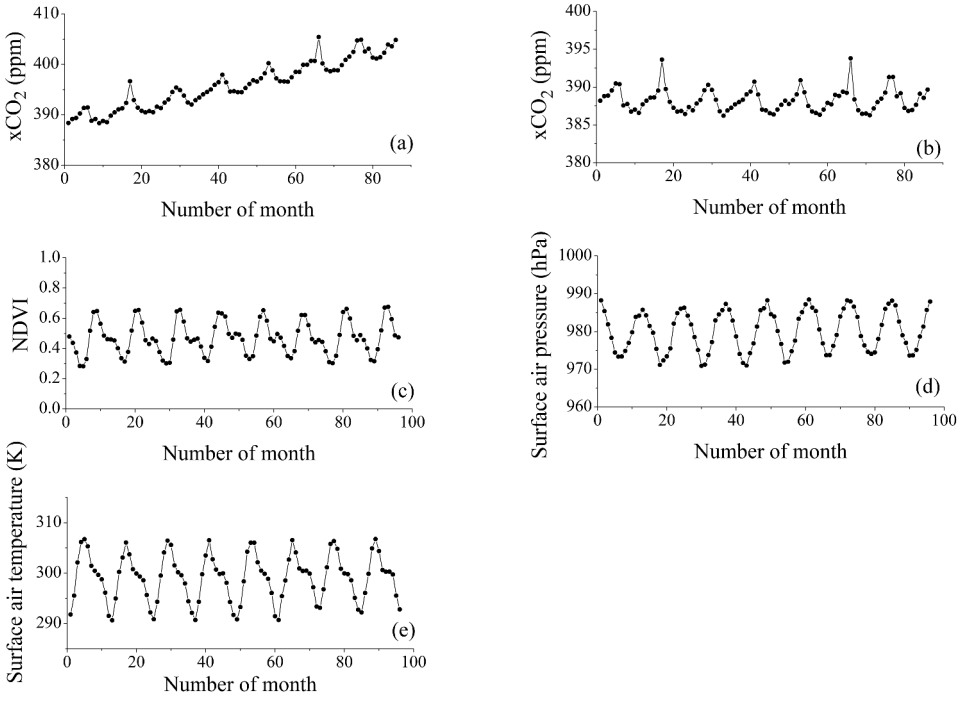

Figure 7. Annual variation of (a) CO_2 concentration, (b) seasonal fluctuation over the initial value of CO_2 concentration, (c) NDVI, (d) surface pressure and (e) surface air temperature for the period of year 2010 to 2017, each parameter averaged over the twenty-five urban areas of.Figure 1, obtained from NASA-Giovanni database specified in Table 1

exists a compliance of the annual variation of the atmospheric pressure due to change in temperature with the annual change of CO_2. Analysing the data of Figures 7(b), 5(c, d) it was found that the NDVI minima almost coincided with the CO_2 maxima and the air pressure minima had a phase shift of few months with the CO_2 maxima. Thus, the NDVI and the atmospheric pressure seemed to have a combined effect on the seasonal variation of CO_2 concentration. However, none of the above periodicities was of any regular waveform and was supposed to comprise more than one periodic component. Their individual roles were identified with the frequency-domain analysis illustrated below.

3.4. Fourier transform analysis

Figure 7 establishes that the seasonal changes of both the NDVI and the atmospheric pressure are related to the seasonal change of CO_2 but none of these two is sufficient alone to explain the phenomena. The increasing phase of NDVI does not synchronize with the decreasing phase of CO_2 so that the carbon uptake period cannot be correlated directly with the vegetation dynamism. Similarly, the annual growth and decay of surface pressure do not coincide with that of CO_2 and there remains a difference of several months between them. The actual role of these parameters is explored more precisely using their Fourier transforms, as depicted below.

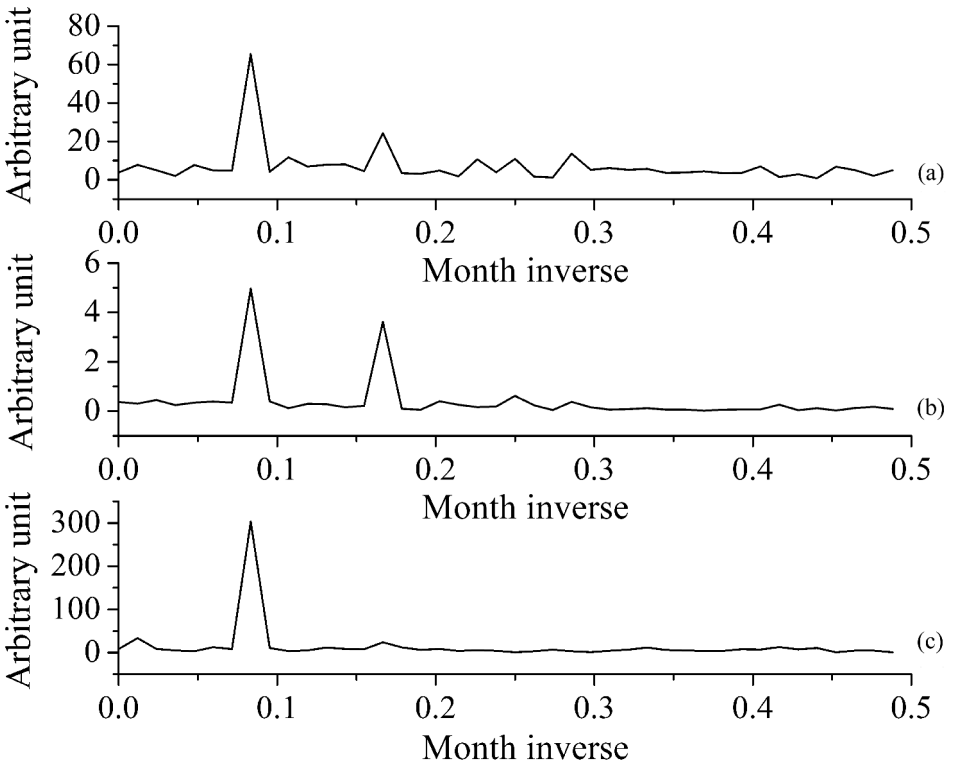

Figure 8. Fourier transform spectra for (a) CO_2, (b) NDVI and (c) surface pressure for areas specified with Figure 7. The arbitrary units indicate the proportional variations of the parameters.

Figure 8 illustrates the Fourier transforms for the temporal variations of CO_2, NDVI, and air pressure for the areas specified in Figure 7. It is noted that the CO_2 variation exhibits a prominent annual and a feeble semi-annual periodicity whereas the NDVI undergoes two prominent periodicities. The atmospheric pressure shows only the annual periodicity. It is inferred from Figures 7 and 8 that the CO_2-NDVI relationship, as expected, is anti-phase for both annual and semi-annual variations so that the increase of one parameter corresponds to the decrease of the other. The CO_2-Pressure interaction is, however, of a different nature. It affects mainly the annual variation and partly the semi-annual variation. In both cases, there exists a phase difference between these two. For the annual variation alone, the effect of surface pressure is more organized than that of NDVI.

3.5. CO_2 redistribution model

As obvious from the above discussions, the periodic change in atmospheric pressure has significant role in causing the annual change in CO_2 concentration. The question is how it causes such change. A possible reason may be the transfer of more surface-level CO_2 to higher altitudes thereby increasing the effective concentration through the whole atmospheric path for the solar radiation. Such possibility corroborates the findings of *El Nino* effect (Keeling, Chin, and Whorf 1996; Nevison et al. 2008; Jiang et al. 2013; Ravi Kumar et al. 2016), where the warm atmosphere corresponds to the growth of CO_2 flux. Since the

spectroscopic technique for assessing atmospheric gas concentration rests on the principle of radiation attenuation through the average gaseous concentration of the total atmospheric path and not that adjacent to the earth surface, the expanding surface-level CO_2 up to higher altitudes contributes more to the attenuation of radiation resulting in higher effective concentration of CO_2. This section demonstrates such a possibility of apparent increase of CO_2 concentration using the results of ground-based spectroradiometric measurements and the redistribution model for CO_2 concentration developed in Section 2.3.

Table 4 compares two different assessments: the directly measured local CO_2 ground-level concentration and the corresponding spectroscopic retrieval of the atmospheric column average of CO_2 concentration at the same site. It is interesting to note that the densely populated, vehicle-congested places having higher ground-level CO_2 concentration do not yield always higher column average of CO_2 concentration. It establishes that the local CO_2 concentration at ground level and that averaged over the whole atmospheric column are two different features. The former one takes long time to get assimilated uniformly in air whereas the latter one, being well mixed with air is subject to instantaneous changes in atmospheric conditions. The theoretical model developed in Section 2.3 quantifies this concept. Figure 9 shows several theoretical curves for CO_2 concentration (ppm) generated with Equations (1), (4) and (8) demonstrating the change in CO_2 vertical concentration profile due to change in air temperature (solid and dotted lines) and the consequent air pressure with different extents of unmixed vertical transport component [$\upsilon(z)$] and other changed parameters (h, σ and χ) indicated in the figures. The figures indicate that the CO_2 vertical profiles may differ widely but the phenomenon of vertical redistribution of molecules takes place irrespective of the presence of the vertical transport component and the effect is more prominent in the lower atmosphere (≤ 5 km).

Figures 2 and 7 may be revisited now in the light of the above explanation for vertical redistribution of atmospheric CO_2. In summer seasons, the higher surface temperature causes the surface pressure to decrease. The decreased surface pressure expands the surface-level air along with the mixed component of CO_2 to higher altitudes thereby

Table 4. CO_2 concentration measured at ground level (with GCH-2018 CO_2 metre) and estimated for atmospheric column average (from ASD spectroradiometry) at different types of sites. Climatic conditions: full sun, temperature 33 to 34°C, humidity 44%, pressure 1007 mbar, wind SW 9 km hr^{-1}.

				Atmospheric average of CO_2 concentration (ppm)	
Ambient condition of the site	Approximate time of measurement	Solar illumination (klux)	Ground- level CO_2 concentration (ppm)	From CO_2-1	From CO_2-2
Less population, less vehicles (suburban area)	09:00 AM	48.0 to 49.2	410 to 412	336 to 337	335 to 336
	10:30 AM	58.0 to 63.0	386	380	390
Dense population, more vehicles (busy road)	11:30 to 11:45 AM	67.2	540 to 542	415 to 417	431 to 432
Car parking lot	12:00 to 12:10 PM	58.0 to 58.2	504 to 505	437 to 438	423 to 424
Grass field of city	01:15 to 01:30 PM	62.0 to 62.5	450 to 453	429 to 431	405 to 406
7^{th} floor rooftop, windy atmosphere	01:30 to 01:45 PM	55.5 to 57.2	390 to 395	400 to 402	412 to 414

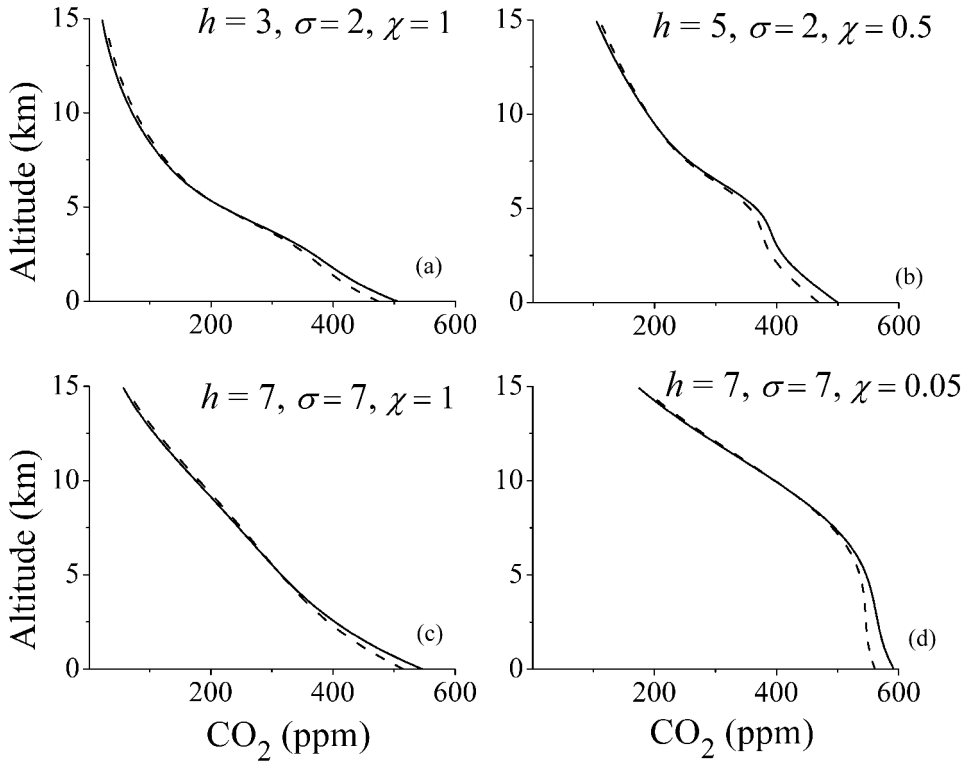

Figure 9. Theoretical curves generated with Equations (1), (4) and (8) demonstrating the change in CO_2 vertical concentration profile due to change in air temperature from 300 K (solid line) to 320 K (dashed line) and the consequent air pressure in presence of different extents of vertical transport component: (a) 10%, (b) 10%, (c) 25% and (d) 50% of ground level concentration and other changed parameters indicated in the figures.

Table 5. Some comparisons of the extent of CO_2 seasonal variation with the possible change due to temperature fluctuation according to Equation (11).

	CO_2 (ppm)		Corresponding temperature (K)		
Referred data	Maximum (n_{01})	Minimum (n_{02})	Maximum (T_{02})	Minimum (T_{02})	Reduced CO_2 (ppm) [Equation (11)]
Figure 2 (*a*): Weak, 2016	411.88	396.28	306.0	301.0	405.15
Figure 2 (*b*): Strong, 2016	399.58	378.76	308.0	304.5	395.04
Figure 2 (*c*): Weak, 2017	411.58	400.40	307.6	300.5	402.08
Figure 2 (*d*): Strong, 2017	400.41	388.84	304.5	302.5	397.78
Figure 7 (*a*)	408.24	398.39	311.6	304.5	398.94

causing more attenuation of radiation through the whole atmospheric path and resulting in an increased effective CO_2 concentration. The change may be as large as the order of the observed seasonal changes. Some examples of such validation are presented in Table 5, which includes the maximum and minimum values of the fitted CO_2 seasonal variation

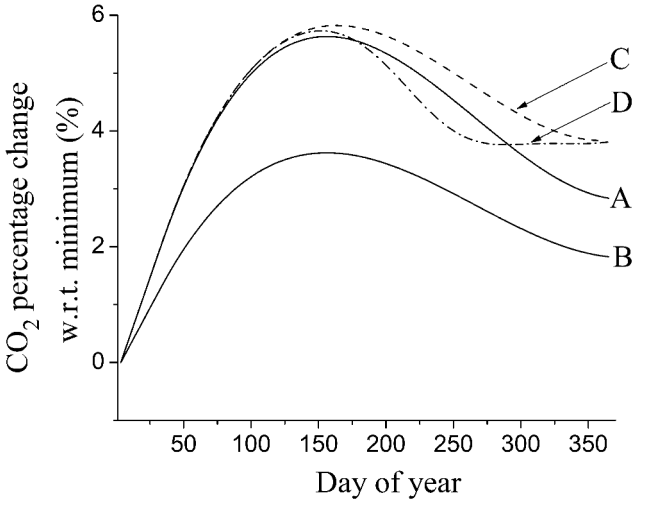

Figure 10. Annual percentage change in seasonal CO_2 concentration simulated with Equation (1) for the vertical profiles of Figure 9 (a) (curve-A) and Figure 9 (d) (curve-D). The dotted lines indicate the trend of variation with annual monotonic increase (curve-C) and with the combination of monotonic increase and vegetation uptake (curve-D).

used in this work with the corresponding mean temperatures. Assuming these maximum and minimum CO_2 values analogous to n_{01} and n_{02}, respectively, of Equation (11) and the temperatures acting as proxy for T_{02} and T_{01} correspondingly, calculations were made for the reduced concentration with increased temperature using Equation (11). It is noted that the maximum values come down to almost of the order of the minimum values. Another validation is presented in Figure 10, where the annual percentage change in seasonal CO_2 concentration is generated with the redistribution model for each day (Section 2.3.1). The curves A and B in Figure 10 correspond to the vertical profiles of Figure 9(a,d), respectively. The extent of seasonal variation in Figure 2 is about 2.5% to 5% so that the simulation in Figure 10 is shown for the same order. The dotted lines indicate how the variation would change with annual monotonic increase (curve-C) and with both monotonic increase and vegetation uptake (curve-D).

The above-discussed theory of vertical redistribution of atmospheric CO_2 molecules under changed condition of temperature and pressure is propounded as an interpretation on the observed seasonal change of CO_2 concentration. It states that whatever may be the nature of the vertical profile, the CO_2 concentration at an arbitrary altitude with respect to that at the ground surface can shift with the variation in temperature and pressure giving rise to an apparent change in spectroscopic results. Since these parameters must be present in some form or other in the climate modelling for global level, one could expect similar seasonal variation for comparable climates.

4. Conclusions

This work investigates the seasonal change of atmospheric CO_2 concentration, identifies the influences of atmospheric pressure and temperature on it and propounds an

illustrative climate model for the same based on vertical redistribution of CO_2 molecules. The study was initiated at the background of a well-known seasonal change of CO_2, a well-accepted reason of vegetation vigour and the mismatch of differed results on the annual variability at different locations with diversified explanations. The work analysed satellite data on the trend of CO_2 seasonal change and its correspondence with vegetation parameters, such as SIF and NDVI and atmospheric pressure and temperature with high temporal resolution data for a specific region and long-term, coarser resolution data over a larger region of tropical, plain, urban area of India. In order to pin-point the periodic changes, the temporal variations were studied in frequency domain also. Ground measurements were carried out to compare the surface-level and atmospheric column-averaged CO_2 concentrations for places of varied urban crowding, which established the separate existence of the local unmixed and the column-averaged air-mixed CO_2 concentrations.

The trend of the annual variation was quantified by identifying the seasonal maximum in summer and tracking the periodic increase and decrease with third order polynomial. The extent of SIF, a representative of carbon uptake by photosynthesis matched the periodicity but could not explain the prominent increase of CO_2 during a year. Thus, the existence of some other factor was predicted. The factors suggested in the previous studies are somehow associated with atmospheric pressure. So this quantity, along with the corresponding temperature data was explored and several features, such as decrease in surface pressure in monsoon/autumn and increase in winter and lowering of pressure while CO_2 increasing indicated a strong influence of atmospheric pressure on CO_2 variation. Both NDVI and atmospheric pressure were found to have a combined effect on the seasonal variation of CO_2 concentration. Each component of variation was identified with frequency-domain analysis.

To explain the mode of air pressure variation affecting the CO_2 seasonal variability, a mathematical model is developed for vertical redistribution of CO_2 molecules under changed conditions of temperature and pressure, which establishes that unlike the vegetation uptake, the pressure change merely redistributes the vertical arrangement of CO_2 molecules. It does not actually remove or introduce any CO_2 but contributes to an apparent change through vertical rearrangement of molecules thereby changing the atmospheric path for radiation absorption. The spectroscopic assessment of gas concentration records the extent of radiation absorption, which depends on the number of molecules in the atmospheric path subject to pressure variation. Whether or not the vertical CO_2 profile changes due to the diffusion of unmixed components, the number density of air-mixed atmospheric CO_2 at an arbitrary altitude can vary with the seasonal alteration of surface air temperature, hence that of the air pressure. The simple model sketched here not only explains the present findings, it is expected to provide with a climate model explaining the atmospheric CO_2 concentration at an arbitrary altitude under the influence of temperature and pressure.

Acknowledgements

The authors thankfully acknowledge the infrastructural supports of Presidency University, Kolkata and Space Applications Centre, Indian Space Research Organization. The use of OCO-2, NASA Giovanni and other data mentioned in the text is also thankfully acknowledged.

Disclosure statement

No potential conflict of interest was reported by the authors.

ORCID

Barun Raychaudhuri http://orcid.org/0000-0002-1718-9415

References

Andrews, A. E., J. D. Kofler, M. E. Trudeau, J. C. Williams, D. H. Neff, K. A. Masarie, D. Y. Chao, et al. 2014. "CO_2, CO, and CH_4 Measurements from Tall Towers in the NOAA Earth System Research Laboratory's Global Greenhouse Gas Reference Network: Instrumentation, Uncertainty Analysis, and Recommendations for Future High-accuracy Greenhouse Gas Monitoring Efforts." *Atmospheric Measurement Techniques* 7 (2): 647–687. doi:10.5194/amt-7-647-2014.

Basu, S., M. Krol, A. Butz, C. Clerbaux, Y. Sawa, T. Machida, H. Matsueda, C. Frankenberg, O. P. Hasekamp, and I. Aben. 2014. "The Seasonal Variation of the CO_2 Flux over Tropical Asia Estimated from GOSAT, CONTRAIL, and IASI." *Geophysical Research Letters* 41 (5): 1809–1815. doi:10.1002/2013GL059105.

Berner, R. A. 2003. "The Long-term Carbon Cycle, Fossil Fuels and Atmospheric Composition." *Nature* 426 (6964): 323–326. doi:10.1038/nature02131.

Bovensmann, H., J. P. Burrows, M. Buchwitz, J. Frerick, S. Noël, V. V. Rozanov, K. V. Chance, and A. P. H. Goede. 1999. "SCIAMACHY: Mission Objectives and Measurement Modes." *Journal of the Atmospheric Sciences* 56 (2): 127–150. doi:10.1175/1520-0469(1999)056<0127:SMOAMM>2.0.CO;2.

Buermann, W., B. R. Lintner, C. D. Koven, A. Angert, J. E. Pinzon, C. J. Tucker, and I. Y. Fung. 2007. "The Changing Carbon Cycle at Mauna Loa Observatory." *Proceedings of the National Academy of Sciences* 104 (11): 4249–4254. doi:10.1073/pnas.0611224104.

Buschmann, M., N. M. Deutscher, V. Sherlock, M. Palm, T. Warneke, and J. Notholt. 2016. "Retrieval of xCO_2 from Ground-based Mid-infrared (NDACC) Solar Absorption Spectra and Comparison to TCCON." *Atmospheric Measurement Techniques* 9: 577–585. doi:10.5194/amt-9-577–2016.

Crisp, D., H. R. Pollock, R. Rosenberg, L. Chapsky, R. A. M. Lee, F. A. Oyafuso, C. Frankenberg, et al. 2017. "The On-orbit Performance of the Orbiting Carbon Observatory-2 (OCO-2) Instrument and Its Radiometrically Calibrated Products." *Atmospheric Measurement Techniques* 10 (1): 59–81. doi:10.5194/amt-10-59-2017.

Crisp, D., R. M. Atlas, F.-M. Breon, L. R. Brown, J. P. Burrows, P. Ciais, B. J. Connor, et al. 2004. "The Orbiting Carbon Observatory (OCO) Mission." *Advances in Space Research* 34 (4): 700–709. doi:10.1016/j.asr.2003.08.062.

Dennison, P. E., A. K. Thorpe, E. R. Pardyjak, D. A. Roberts, Y. Qi, R. O. Green, E. S. Bradley, and C. C. Funk. 2013. "High Spatial Resolution Mapping of Elevated Atmospheric Carbon Dioxide Using Airborne Imaging Spectroscopy: Radiative Transfer Modeling and Power Plant Plume Detection." *Remote Sensing of Environment* 139: 116–129. doi:10.1016/j.rse.2013.08.001.

Dettinger, M. D., and M. Ghil. 1998. "Seasonal and Interannual Variations of Atmospheric CO2 and Climate." Tellus B 50 (1): 1–24. doi:10.1034/j1600-0889.1998.00001.x

Diallo, M., B. Legras, E. Ray, A. Engel, and J. A. Añel. 2017. "Global Distribution of CO_2 in the Upper Troposphere and Stratosphere." *Atmospheric Chemistry and Physics* 17 (6): 3861–3878. doi:10.5194/acp-17-3861-2017.

Elachi, C., and J. van Zyl. 2006. *Introduction to the Physics and Techniques of Remote Sensing*. *2nd* ed. New Jersey & Canada: John Wiley & Sons.

Frankenberg, C., C. O'Dell, L. Guanter, and J. McDuffie. 2012. "Remote Sensing of Near-infrared Chlorophyll Fluorescence from Space in Scattering Atmospheres: Implications for Its Retrieval and

Interferences with Atmospheric CO_2 Retrievals." *Atmospheric Measurement Techniques* 5 (8): 2081–2094. doi:10.5194/amt-5-2081-2012.

Frankenberg, C., R. Pollock, R. A. M. Lee, R. Rosenberg, J. F. Blavier, D. Crisp, C. W. O'Dell, et al. 2015. "The Orbiting Carbon Observatory (OCO-2): Spectrometer Performance Evaluation Using Pre-launch Direct Sun Measurements." *Atmospheric Measurement Techniques* 8 (1): 301–313. doi:10.5194/amt-8-301-2015.

Fu, Z., J. Dong, Y. Zhou, P. C. Stoy, and S. Niu. 2017. "Long Term Trend and Interannual Variability of Land Carbon Uptake – The Attribution and Processes." *Environmental Research Letters* 12 (1): 014018. doi:10.1088/1748-9326/aa5685.

Gamon, J. A., C. B. Field, M. L. Goulden, K. L. Griffin, A. E. Hartley, G. Joel, J. Penuelas, and R. Valentini. 1995. "Relationships between NDVI, Canopy Reflectance, and Photosynthesis in Three Californian Vegetation Types." *Ecological Applications* 5 (1): 28–41. doi:10.2307/1942049.

Green, R. O. 2001. "Measuring the Spectral Expression of Carbon Dioxide in the Solar Reflected Spectrum with AVIRIS." Proceedings of the 11th annual Airborne Earth Science Workshop. Pasadena, CA: Jet Propulsion Laboratory.

Gupta, A., S. K. Dhaka, Y. Matsumi, R. Imasu, S. Hayashida, and V. Singh. 2019. ""Seasonal and Annual Variation of AIRS Retrieved CO_2 over India during 2003–2011." *Journal of Earth System Science* 128: 92. doi:10.1007/s12040-019-1108-7.

Hakkarainen, J., I. Ialongo, and J. Tamminen. 2016. "Direct Space-based Observations of Anthropogenic CO_2 Emission Areas from OCO-2." *Geophysical Research Letters* 43 (21): 11–400. doi:10.1002/2016GL070885.

Hamazaki, T., Y. Kaneko, and A. Kuze. 2004. "Carbon Dioxide Monitoring from the GOSAT Satellite." Proceedings of XXth ISPRS Conference VII, pp. 225–227, Istanbul, Turkey, 12-13 July 2004.

Huang, H., T. Wang, R. Talbot, M. Xie, H. Mao, S. Li, B. Zhuang, et al. 2015. "Temporal Characteristics of Atmospheric CO_2 in Urban Nanjing, China." *Atmospheric Research* 153: 437–450. doi:10.1016/j.atmosres.2014.09.007.

Imasu, R., and Y. Tanabe. 2018. "Diurnal and Seasonal Variations of Carbon Dioxide (CO_2) Concentration in Urban, Suburban, and Rural Areas around Tokyo." *Atmosphere* 9 (10): 367. doi:10.3390/atmos9100367.

Jiang, X., D. Crisp, E. T. Olsen, S. S. Kulawik, C. E. Miller, T. S. Pagano, M. Liang, and Y. L. Yung. 2016. "CO_2 Annual and Semiannual Cycles from Multiple Satellite Retrievals and Models." *Earth and Space Science* 3 (2): 78–87. doi:10.1002/2014EA000045.

Jiang, X., J. Wang, E. T. Olsen, M. Liang, T. S. Pagano, L. L. Chen, S. J. Licata, and Y. L. Yung. 2013. "Influence of El Nino on Midtropospheric CO_2 from Atmospheric Infrared Sounder and Model." *Journal of the Atmospheric Sciences* 70 (1): 223–230. doi:10.1175/JAS-D-11-0282.1.

Joiner, J., Y. Yoshida, A. P. Vasilkov, K. Schaefer, M. Jung, L. Guanter, Y. Zhang, et al. 2014. "The Seasonal Cycle of Satellite Chlorophyll Fluorescence Observations and Its Relationship to Vegetation Phenology and Ecosystem Atmosphere Carbon Exchange." *Remote Sensing of Environment* 152: 375–391. doi:10.1016/j.rse.2014.06.022.

Keeling, C. D., S. C. Piper, R. B. Bacastow, M. Wahlen, T. P. Whorf, M. Heimann, and H. A. Meijer. 2005. "Atmospheric CO_2 and $^{13}CO_2$ Exchange with the Terrestrial Biosphere and Oceans from 1978 to 2000: Observations and Carbon Cycle Implications." In *A History of Atmospheric CO_2 and Its Effects on Plants, Animals, and Ecosystems*, edited by I. T. Baldwin, M. M. Caldwell, G. Heldmaier, R. Jackson, O. L. Lange, H. A. Mooney, E. D. Schulze, et al., 83–113. New York: Springer.

Keeling, C. D., J. F. S. Chin, and T. P. Whorf. 1996. "Increased Activity of Northern Vegetation Inferred from Atmospheric CO2 Measurements." *Nature* 382 (6587): 146–149. doi:10.1038/382146a0.

Keeling, C. D., R. B. Bacastow, A. E. Bainbridge, C. A. Ekdahl Jr, P. R. Guenther, L. S. Waterman, and J. F. S. Chin. 1976. "Atmospheric Carbon Dioxide Variations at Mauna Loa Observatory, Hawaii." *Tellus* 28 (6): 538–551.

Kondratyev, K. Y., and C. Varotsos. 1995. "Atmospheric Greenhouse Effect in the Context of Global Climate Change." *Il Nuovo Cimento C* 18 (2): 123–151. doi:10.1007/BF02512015.

Krapivin, V. K., and C. A. Varotsos. 2016. "Modelling the CO2 Atmosphere-ocean Flux in the Upwelling Zones Using Radiative Transfer Tools." *Journal of Atmospheric and Solar–Terrestrial Physics* 150: 47–54. doi:10.1016/j.jastp.2016.10.015.

Kuze, A., H. Suto, M. Nakajima, and T. Hamazaki. 2009. "Thermal and near Infrared Sensor for Carbon Observation Fourier-transform Spectrometer on the Greenhouse Gases Observing Satellite for Greenhouse Gases Monitoring." *Applied Optics* 48 (35): 6716–6733. doi:10.1364/AO.48.006716.

Lee, E., F. W. Zeng, R. D. Koster, B. Weir, L. E. Ott, and B. Poulter. 2018. "The Impact of Spatiotemporal Variability in Atmospheric CO_2</sub> Concentration on Global Terrestrial Carbon Fluxes." *Biogeosciences* 15 (18): 5635–5652. doi:10.5194/bg-15-5635-2018.

Li, K., F., . B. Tian, D. E. Waliser, and Y. L. Yung. 2010. "Tropical Mid-tropospheric CO_2 Variability Driven by the Madden–Julian Oscillation." *Proceedings of the National Academy of Sciences* 107 (45): 19,171–19,175. doi:10.1073/pnas.1008222107/-/DCSupplemental.

Li, Z., J. Xia, A. Ahlström, A. Rinke, C. Koven, D. J. Hayes, D. Ji, et al. 2018. "Non-uniform Seasonal Warming Regulates Vegetation Greening and Atmospheric CO_2 Amplification over Northern Lands." *Environmental Research Letters* 13 (12): 124008. doi:10.1088/1748-9326/aae9ad.

Machida, T., H. Matsueda, Y. Sawa, Y. Nakagawa, K. Hirotani, N. Kondo, K. Goto, T. Nakazawa, K. Ishikawa, and T. Ogawa. 2008. "Worldwide Measurements of Atmospheric CO2 and Other Trace Gas Species Using Commercial Airlines." *Journal of Atmospheric and Oceanic Technology* 25 (10): 1744–1754. doi:10.1175/2008JTECHA1082.1.

Marescaux, A., V. Thieu, A. V. Borges, and J. Garnier. 2018. "Seasonal and Spatial Variability of the Partial Pressure of Carbon Dioxide in the Human-impacted Seine River in France." *Scientific Reports* 8 (1): 13961. doi:10.1038/s41598-018-32332-2.

Miao, G., K. Guan, X. Yang, C. J. Bernacchi, J. A. Berry, E. H. DeLucia, J. Wu, et al. 2018. "Sun-induced Chlorophyll Fluorescence, Photosynthesis, and Light Use Efficiency of a Soybean Field from Seasonally Continuous Measurements." *Journal of Geophysical Research: Biogeosciences* 123 (2): 610–623. doi:10.1002/2017JG004180.

Monfray, P., A. Gaudry, G. Polian, and G. Lambert. 1987. "Seasonal Variations of Atmospheric CO_2 in the Southern Indian Ocean." *Tellus B: Chemical and Physical Meteorology* 39 (1–2): 67–71. doi:10.3402/tellusb.v39i1-2.15323.

Nestola, E., C. Calfapietra, C. A. Emmerton, C. Wong, D. R. Thayer, and J. A. Gamon. 2016. "Monitoring Grassland Seasonal Carbon Dynamics, by Integrating MODIS NDVI, Proximal Optical Sampling, and Eddy Covariance Measurements." *Remote Sensing* 8 (3): 260. doi:10.3390/rs8030260.

Nevison, C. D., N. M. Mahowald, S. C. Doney, I. D. Lima, G. R. Van der Werf, J. T. Randerson, D. F. Baker, P. Kasibhatla, and G. A. McKinley. 2008. "Contribution of Ocean, Fossil Fuel, Land Biosphere, and Biomass Burning Carbon Fluxes to Seasonal and Interannual Variability in Atmospheric CO_2." *Journal of Geophysical Research: Biogeosciences* 113 (G1): G01010. doi:10.1029/2007JG000408.

Piao, S., Z. Liu, Y. Wang, P. Ciais, Y. Yao, S. Peng, F. Chevallier, et al. 2018. "On the Causes of Trends in the Seasonal Amplitude of Atmospheric CO_2." *Global Change Biology* 24 (2): 608–616. doi:10.1111/gcb.13909.

Queißer, M., M. Burton, and R. Kazahaya. 2019. "Insights into Geological Processes with CO_2 Remote Sensing – A Review of Technology and Applications." *Earth Science Reviews* 188: 389–426. doi:10.1016/j.earscirev.2018.11.016.

Ravi Kumar, K., J. V. Revadekar, and Y. K. Tiwari. 2014. "AIRS Retrieved CO2 and Its Association with Climatic Parameters over India during 2004–2011." *Science of the Total Environment* 476–477: 79–89. doi:10.1016/j.scitotenv.2013.12.118.

Ravi Kumar, K., Y. K. Tiwari, J. V. Revadekar, R. Vellore, and T. Guha. 2016. "Impact of ENSO on Variability of AIRS Retrieved CO_2 over India." *Atmospheric Environment* 142: 83–92. doi:10.1016/j.atmosenv.2016.07.001.

Román-Cascón, C., C. Yagüe, J. A. Arrillaga, M. Lothon, E. R. Pardyjak, F. Lohou, R. M. Inclán, et al. 2019. "Comparing Mountain Breezes and Their Impacts on CO_2 Mixing Ratios at Three Contrasting Areas." *Atmospheric Research* 221: 111–126. doi:10.1016/j.atmosres.2019.01.019.

Sawyer, J. S. 1972. "Man-made Carbon Dioxide and the "Greenhouse" Effect." *Nature* 239: 23–26. doi:10.1038/239023a0.

Stockie, J. M. 2011. "The Mathematics of Atmospheric Dispersion Modelling." *SIAM Review* 53 (2): 349–372. doi:10.1137/10080991X.

Sun, Y., C. Frankenberg, M. Jung, J. Joiner, L. Guanter, P. Kohler, and T. Magney. 2018. "Overview of Solar-Induced Chlorophyll Fluorescence (SIF) from the Orbiting Carbon Observatory-2: Retrieval,

Cross-mission Comparison, and Global Monitoring for GPP." *Remote Sensing of Environment* 209: 808–823. doi:10.1016/j.rse.2018.02.016.

Tiwari, Y. K., J. V. Revadekar, and K. Ravi Kumar. 2013. "Variations in Atmospheric Carbon Dioxide and Its Association with Rainfall and Vegetation over India." *Atmospheric Environment* 68: 45–51. doi:10.1016/j.atmosenv.2012.11.040.

Tiwari, Y. K., R. K. Vellore, K. Ravi Kumar, M. van der Schoot, and C. H. Cho. 2014. "Influence of Monsoons on Atmospheric CO_2 Spatial Variability and Ground-based Monitoring over India." *Science of the Total Environment* 490: 570–578. doi:10.1016/j.scitotenv.2014.05.045.

Umezawa, T., H. Matsueda, Y. Sawa, Y. Niwa, T. Machida, and L. Zhou. 2018. "Seasonal Evaluation of Tropospheric CO 2 over the Asia-Pacific Region Observed by the CONTRAIL Commercial Airliner Measurements." *Atmospheric Chemistry and Physics* 18 (20): 14851–14866. doi:10.5194/acp-18-14851–2018.

Varotsos, C., M.-N. Assimakopoulos, and M. Efstathiou. 2007. "Technical Note: Long-term Memory Effect in the Atmospheric CO_2</sub> Concentration at Mauna Loa." *Atmospheric Chemistry and Physics* 7 (3): 629–634. doi:10.5194/acpd-6-11957-2006.

Watanabe, H., K. Hayashi, T. Saeki, S. Maksyutov, I. Nasuno, Y. Shimono, Y. Hirose, et al. 2015. "Global Mapping of Greenhouse Gases Retrieved from GOSAT Level 2 Products by Using a Kriging Method." *International Journal of Remote Sensing* 36 (6): 1509–1528. doi:10.1080/01431161.2015.1011792.

Wei, J., A. Savtchenko, B. Vollmer, T. Hearty, A. Albayrak, D. Crisp, and A. Eldering. 2014. "Advances in CO_2 Observations from AIRS and ACOS." *IEEE Geoscience and Remote Sensing Letters* 11: 891–895. doi:10.1109/LGRS.2013.2281147.

Wunch, D., G. C. Toon, J. F. L. Blavier, R. A. Washenfelder, J. Notholt, B. J. Connor, D. W. T. Griffith, V. Sherlock, and P. O. Wennberg. 2011. "The Total Carbon Column Observing Network." *Philosophical Transactions of the Royal Society A: Mathematical, Physical and Engineering Sciences* 369 (1943): 2087–2112. doi:10.1098/rsta.2010.0240.

Wunch, D., P. O. Wennberg, G. Osterman, B. Fisher, B. Naylor, C. M. Roehl, C. O'dell, et al. 2017. "Comparisons of the Orbiting Carbon Observatory-2 (OCO-2) X_{CO2} Measurements with TCCON." *Atmospheric Measurement Techniques* 10 :2209–2238. doi:10.5194/amt-2016-227.

Xueref-Remy, I., E. Dieudonné, C. Vuillemin, M. Lopez, C. Lac, M. Schmidt, M. Delmotte, et al. 2018. "Diurnal, Synoptic and Seasonal Variability of Atmospheric CO_2 in the Paris Megacity Area." *Atmospheric Chemistry and Physics* 18 :3335–3362. doi:10.5194/acp-18-3335-2018.

Yoshida, Y., Y. Ota, N. Nawo Eguchi, K. N. Kikuchi, H. Tran, I. Morino, and T. Yokota. 2011. "Retrieval Algorithm for CO_2 and CH_4 Column Abundances from Short-wavelength Infrared Spectral Observations by the Greenhouse Gases Observing Satellite." *Atmospheric Measurement Techniques* 4 (4): 717–734. doi:10.5194/amt-4-717-2011.

Zhang, X., K. R. Gurney, P. Rayner, D. Baker, and Y.-P. Liu. 2016. "Sensitivity of Simulated CO_2 Concentration to Sub-annual Variations in Fossil Fuel CO_2 Emissions." *Atmospheric Chemistry & Physics* 16 (4): 1907–1918. doi:10.5194/acp-16-1907-2016.

Zhao, F., and N. Zeng. 2014. "Continued Increase in Atmospheric CO_2 Seasonal Amplitude in the 21st Century Projected by the CMIP5 Earth System Models." *Earth System Dynamics* 5 (2): 423–439. doi:10.5194/esd-5-423-2014.